

1 **Monster potential meets potential monster; the pros and cons of deploying**
2 **genetically modified microalgae for biofuels production**

3 K.J. Flynn^{1,*}, A. Mitra¹, H.C. Greenwell² and J.Sui¹

4

5 1) Centre of Sustainable Aquatic Research, Swansea University, Swansea SA2 8PP, U.K.

6 2) Department of Earth Sciences, Durham University, Durham DH1 3LE, U.K.

7

8 **ABSTRACT**

9 Biofuels production from microalgae attracts much attention but remains an unproven
10 technology. We explore routes to enhance production through modifications to a range of
11 generic microalgal physiological characteristics. Our analysis shows that biofuels production
12 may be enhanced ca. 5 fold through genetic modification (GM) of factors affecting growth
13 rate, respiration, photoacclimation, photosynthesis efficiency and the minimum cell quotas for
14 nitrogen and phosphorous (N:C and P:C). However, simulations indicate that the ideal GM
15 microalgae for commercial deployment could, on escape to the environment, become a
16 harmful algal bloom species *par excellence*, with attendant risks to ecosystems and
17 livelihoods. In large measure this is because an organism able to produce carbohydrate and/or
18 lipid at high rates, providing stock metabolites for biofuels production, will also be able to
19 attain a stoichiometric composition that will be far from optimal as food for the support of
20 zooplankton growth. This composition could suppress or even halt the grazing activity that
21 would otherwise control the microalgal growth in nature. In consequence we recommend that
22 the genetic manipulation of microalgae, with inherent consequences on a scale comparable to
23 geoengineering, should be considered under strict international regulation.

24

25 1. INTRODUCTION

26 The production of liquid transport biofuels from terrestrial crop plants is a proven
27 technology (Smith *et al.* 2009) that continues to attract controversy. Much concern is levelled
28 at the comparative societal, ethical and political values of using land and fertilizer for energy
29 rather than feeding populaces. An alternative to the use of photosynthetic higher plants is to
30 use photosynthetic microalgae. The term “microalgae” typically describes any photosynthetic
31 microbe, either prokaryotic cyanobacteria or eukaryotic protists. While some of these
32 organisms are capable of synthesising biochemical precursors for biofuels heterotrophically
33 (Chen *et al.* 2011), net C-fixation requires a predominately photosynthetic metabolism under
34 conditions of adequate illumination and (usually) inorganic nutrients. It is these
35 photosynthetic microalgae that we consider here. Microalgae have been suggested to be ideal
36 organism for biofuels production owing to their rapid growth rate, high oil content, suitability
37 for growth on marginal land, and no direct conflict with the growth of food crops (Chisti
38 2007; Wijffels & Barbosa 2010). However, the path to successful deployment of microalgal
39 biofuels is most challenging (Greenwell *et al.* 2010), with the cost estimates for production
40 currently far exceeding fossil fuel prices (Williams & Laurens 2010; Shirvani *et al.* 2011).

41 Irrespective of the form of biofuels produced from microalgae, the objective is to
42 transfer the normal flow of newly fixed carbon (C), from generating structural biomass,
43 towards the accumulation of energy dense C storage products (starch, lipid). While nutrient
44 (especially nitrogen, N) limitation prior to crop harvesting is needed to optimise biofuels
45 production, light limitation is a far more likely event at this stage of microalgae crop growth
46 owing to the self-shading properties of dense, highly pigmented, microalgal suspensions
47 (Flynn *et al.* 2010). As with all commercial crops, approaches to overcoming such inherent
48 limitations to production have attracted considerable interest (Beer *et al.* 2009; Li *et al.* 2010;
49 Radakovits *et al.* 2010).

50 In this work we consider various issues associated with the advantages and
51 disadvantages of applying genetic modification (GM) to microalgae to enhance biofuels
52 production. Similar arguments to those we present here apply to any manipulation of the
53 phenotypic characteristics of microalgae; we use the term genetic modification (GM) to imply
54 any alteration of wild-type characteristics (e.g., Courchesne *et al.* 2009) that would not likely
55 occur naturally. Since these organisms are single-celled microbes with minimum generation
56 times of less than a day, they may be considered more readily amenable to GM than are
57 higher plants. However, it is worth noting that in reality the path to GM of these organisms is
58 far from trivial (Beer *et al.* 2009; Courchesne *et al.* 2009).

59 While deployment of GM biofuels-optimised microalgae may appear to offer great
60 potential, there are counters to this promise. While microalgae in nature, as phytoplankton, are
61 important components of the trophic web leading to fisheries, one may question whether
62 microalgae optimised for biofuels production would readily fit benignly into ecology, or
63 whether they may form harmful algal blooms (HABs). The large-scale growth of
64 microorganisms that can be readily transferred across and between continents (e.g., with
65 migrating wildfowl, or in the ballast water of ships (Hallegraeff 1998)) thus warrants careful
66 consideration.

67 We have conducted our analysis through screening *in silico* GM algal populations,
68 avoiding the attendant environmental and ethical risks of *in vivo* trials. *In silico* models of
69 algal community physiology, though widely used in many oceanographic scenarios (e.g.,
70 Fasham *et al.* 2006), and deployed for simulations of microalgal biomass production (Flynn *et al.*
71 *et al.* 2010), have hitherto not been applied in earnest to examine algal biofuels production.
72 Here, we use a variant of a well documented algal physiology model (Flynn 2001, 2008a;
73 Flynn *et al.* 2010) to investigate options for enhancing microalgal biofuels production through
74 GM routes. We then take the resultant biofuels-optimised GM organism and consider the
75 implications for predator-prey interactions if such an organism escaped into the natural
76 environment. The results indicate that the configuration of a biofuels-optimised organism also
77 describes an organism that, on escape to the natural environment, has the potential to form
78 harmful algae blooms (HABs) on a scale greater than do naturally occurring species.

79

80 **2. METHODS**

81 **2.1 Base algal model**

82 All models represent a compromise between complexity and computational load. The
83 model used here is broadly typical of the more complex examples of mechanistic adaptive
84 microalgal models. The model describing the growth of microalgae was developed from a
85 long line of models (Flynn 2001, 2003). This model type has a firm basis in physiology, and
86 has been well validated in its performance against data for various phytoplankton species,
87 growing under different conditions and various combinations of light, N, P, Fe, and/or Si
88 limitation (Flynn 2001; John & Flynn 2002; Flynn 2003; Fasham *et al.* 2006; Flynn 2008a,
89 2008b; Flynn *et al.* 2008). The implementation here included a description of the interactions
90 between light, nitrogen (N) and phosphorus (P), with photoacclimation according to the
91 “Flynn-Geider” configuration described in Flynn *et al.* (2001).

92 Algal-C was allocated to nitrogenous components (protein and nucleic acids), and
 93 non-nitrogenous structural components, with the balance as surplus C attributed to
 94 components for potential exploitation as biofuels. The simulated contribution to biofuels
 95 material is calculated by reference to the cellular C:N ratio, and the absolute minimum
 96 cellular C:N (CN_{\min}), using the following equation.

$$97 \quad Cex_C = \frac{CN_{cell} - CN_{\min}}{CN_{cell}} = \frac{CN_{cell} - (CN_{core} + Cstruc_N)}{CN_{cell}} \quad (1)$$

98 The value of CN_{\min} can be determined experimentally from N-replete ammonium
 99 grown microalgae. It comprises two main components; the C:N of the core cellular
 100 nitrogenous components (CN_{core}) which is primarily protein and nucleic acids, and the non-
 101 nitrogenous structural material (primarily membranes and cell wall) which is described here
 102 as a C:N value referenced to the N in the core ($Cstruc_N$). The value of CN_{core} is estimated to
 103 have a value of ca. 3.2 gC (gN)^{-1} , from the C:N value of protein and nucleic acids, and the
 104 contribution that these two make to the whole cell (Geider & La Roche 2002). $Cstruc_N$ is
 105 given as $CN_{\min} - CN_{core}$; the typical value of CN_{\min} is around 4 (Geider & La Roche 2002;
 106 Flynn 2008a), yielding a value of this non-nitrogenous $Cstruc_N$ in nutrient-replete cells of 0.8
 107 gC (gN)^{-1} . The biochemical fractionation between different carbohydrates, fatty acids and
 108 lipids within the surplus C (Cex_C) is not described further within the model because there are
 109 insufficient data as yet to support such a development. The fractionation does not affect the
 110 central conclusions of our analysis (considered further in Discussion).

111

112 **2.2. non-GM and GM configurations**

113 The microalgal model described interactions between light (including
 114 photoacclimation), nutrients (N and P) and growth. The base (non-GM) model was configured
 115 to represent a typical microalgae with respect to C:N:P:Chl (Flynn 2001, 2008), and produces
 116 maximum simulated areal production rates similar to peak values in nature (ca. $4 \text{ gC m}^{-2} \text{ d}^{-1}$)
 117 (Sarmiento & Gruber 2006). The default values of constants used for the non-GM
 118 configuration, and the ranges explored for GM configurations, are given in table 1. These are
 119 all phenotypic features for which there are, likely, many genotypic regulators. For example,
 120 altering the photosystem antenna size (Melis 2009) affects phenotypic features of the initial
 121 slope of the photosynthesis-irradiance curve (α^{Chl}) and also, depending on how the cell
 122 responds by altering the number of photosynthesis reaction centres, potentially the maximum
 123 pigment content ($ChlC_{\max}$). An explanation of the features considered is given below.

124

125 **2.2.1 Maximum growth rate (μ_{\max}).** This sets the maximum possible growth rate under
126 optimal conditions. The maximum growth rate attainable in simulations was less than μ_{\max}
127 because growth was simulated in a light-dark cycle (see below). Engineering factors affecting
128 this feature may require a consideration of the source wild-type cell line, cell cycle controls,
129 and limitations on respiratory functions affecting synthesis and cell maintenance (Flynn
130 2009).

131
132 **2.2.2 Respiration rates (basal and metabolic respiration).** Basal respiration (BasRes;
133 described here as a proportion of μ_{\max}) includes that associated with cell maintenance, while
134 metabolic respiration (ProtRes; described here as C respired for the assimilation of N from
135 intracellular ammonium into protein and nucleic acids) is associated with new net synthesis of
136 structural components. Added to respiration is the cost of reducing nitrate to ammonium
137 before assimilating nitrate-N (equivalent to 1.71 gC per g nitrate-N (Flynn & Hipkin 1999)).
138 Engineering a decrease in respiratory costs may require a consideration of features such as
139 protein turnover rates and functioning of key biochemical pathways.

140
141 **2.2.3 ChlC_{max}.** This sets the maximum pigment content, described here as chlorophyll per
142 unit of cell-C. In crude terms this limits the “greenness” of the individual cell. With
143 decreasing light, notably due to self-shading within the cell suspension, photoacclimation
144 within the cell stimulates an increase in photopigment content, to capture more photons for
145 the individual cell. Through natural selection the value of ChlC_{max} is expected to become
146 elevated (Flynn *et al.* 2010), attaining as much as 0.08 g Chl_a (g cell-C)⁻¹ (Anning *et al.*
147 2000). However, such elevated levels cause internal self-shading and critically also self-
148 shading at the population level which decreases efficiency for photosynthesis, and hence
149 decreases overall production. Total productivity is enhanced greatly if the level of
150 photoacclimation (the value of ChlC_{max}) is limited, though this is unlikely to be a stable
151 selective trait (Flynn *et al.* 2010). Engineering this feature may require a consideration of
152 altering photosystem antenna size (Beckmann *et al.* 2009) and/or the number of
153 photosynthetic reaction centres.

154
155 **2.2.4 α^{Chl} .** This phenotypic feature affects the overall efficiency of the light-chemistry
156 conversion process, with units of gC (mol photon)⁻¹ × (m² g⁻¹ Chl). The rate of photosynthesis
157 is thus a function of the available light, the pigment content (ChlC; section 2.2.3) and the

158 value of α^{Chl} ; for further information see Geider *et al.* (1998), Flynn *et al.* (2001) and Flynn
159 (2001, 2003). Various factors affect the value of α^{Chl} , including the photochemistry within the
160 Z-scheme, and the level of self-shading within the cell (MacIntyre *et al.* 2002). Internal self-
161 shading is affected by the antenna size (Chl per reaction centre), overall Chl:C (affected by
162 ChlC_{max}), and cell size. The fundamental basis of life on Earth is thought to have been fixed
163 some 2Ga ago (Shi *et al.* 2005), with natural selection then optimising the packaging of these
164 key biochemical processes. Accordingly, enhancing the efficiency of the basis of
165 photochemistry, a fundamental feature of cell biochemistry, would literally be a real life-
166 changing event.

167

168 **2.2.5 Photoacclimation rate (M).** This is described by parameter M in Flynn *et al.* (2001),
169 and affects the rate at which pigment content is up-regulated with photoacclimation when the
170 illumination falls (see above on ChlC_{max}). Here, the most important feature affected by this
171 rate was the increase in Chl:C on entry into the dark phase of the diel light-dark cycle.
172 Engineering this feature would require modifying the acclimation response rate to darkness
173 and/or to C-limitation.

174

175 **2.2.6 NC_0 and KQN.** These parameters, respectively, describe the minimum cellular N:C (the
176 subsistence quota for N (Flynn 2008a)) and the efficiency of N utilisation (specifically the
177 efficiency of the action of biosynthetic pathways associated with N-compounds (Flynn 2008a,
178 2008b)). Lowering NC_0 would also, most likely, involve a decreased need for basal
179 respiration (i.e., a lowering of protein turnover and damage-repair activities, with a decreased
180 need for associated proteins/enzymes and RNA), and a lowering of the DNA content.
181 Evidence from past experimental studies indicates that KQN sets a linear relationship between
182 cellular N:C and growth rate (Flynn 2008a, 2008b). To decrease KQN, to make the
183 relationship between N:C and growth rate curvi-linear, would require a fundamental change in
184 protein and enzyme synthesis and efficiencies of their operation.

185

186 **2.2.7 PC_0 and KQP.** These are the P counterparts to NC_0 and KQN. There is far greater
187 variability in these parameter values than for NC_0 and KQN, and they are recognised as
188 important features in competition between microalgae (Lui *et al.*, 2001; Flynn 2002). Because
189 of the mixed structural and energetic/regulatory functions of P (contrasting with the mainly
190 structural functions of N), the value of KQP is much lower than KQN, and the resultant often
191 strongly curvi-linear relationship between P:C and growth rate indicates that the cells alter the

192 efficiency of P usage as P becomes limiting (Flynn 2008a, 2008b). To engineer changes in
193 PC_0 and KQP would require decreasing the content of P-containing structural components
194 (DNA, RNA, membranous phospholipids), and enhance the efficiency of use for the
195 remainder.

196

197 **2.2.8 CN_{core} and $Cstruc_N$.** These parameters, respectively, describe the ratio by mass of the
198 nitrogenous material in the cell (as C:N, comprising proteins, DNA and RNA) and the amount
199 of organic non-nitrogenous structural material relative to the nitrogenous component (as C:N,
200 comprising cell wall, membranes); see text associated with equation (1), above. To engineer
201 changes in CN_{core} would require a decrease in the amount of DNA and RNA (as these contain
202 a lower C:N than does protein (Geider & La Roche 2002)), if not a complete rebuild of the
203 very nature of the biochemistry of life. Cell walls in microalgae are not as substantial as those
204 in higher plants, so most of the material in $Cstruc_N$ comprises membranes containing
205 phospholipids. Decreasing $Cstruc_N$ is thus likely to decrease PC_0 . Default values used here
206 are: $CN_{core} = 3.2$; $Cstruc_N = 0.8$ (see Section 2.1).

207

208 **2.3 Microalgal simulations**

209 Growth was simulated with illumination conditions for a cloudless mid summer's day
210 at latitude 0° . An astrological function was used describing the sigmoidal day-light variation
211 with a noon maximum instantaneous photon flux density of $2180 \mu\text{mol m}^{-2} \text{s}^{-1}$ and,
212 accounting for reflectance off the water surface with changing sunlight incidence, giving a
213 day average of $675 \mu\text{mol m}^{-2} \text{s}^{-1}$. It was assumed that conditions of temperature, CO_2 and pH
214 were optimal throughout. The macro-nutrient regime was either that of f/2 (Guillard & Ryther
215 1962) with inorganic N available at $880 \mu\text{M}$ and phosphate at $36.2 \mu\text{M}$, or at some multiple of
216 those concentrations (e.g., $5 \times \text{f}/2$). Simulations to explore optimal configurations of growth
217 and phenotype characteristics were run to steady-state in chemostat-style conditions,
218 assuming a homogeneous distribution of cells over an optical depth of 0.1m, a depth shown
219 previously to be in the optimal range to balance areal and volumetric production rates (Flynn
220 *et al.* 2010). Physico-chemical limitations to the supply of nutrients (including CO_2 injection
221 and the maintenance of pH) were assumed to have been overcome.

222 Areal production is reported for biomass and biofuels (with units of $\text{gC m}^{-2} \text{d}^{-1}$). As
223 simulations were run in chemostat-style, steady-state mode, dilution rates in the plots equate
224 to day-averaged growth rates. The biofuels component represents a portion of biomass,
225 ranging typically from near zero to ca. 70% of the C-biomass, as according to equation 1.

226

227 **2.4 Predator-prey simulations**

228 For the predator-prey simulations, the base (non-GM) configured microalga or its
229 GM-configured counterpart (table 2) were simulated as being grown together with a
230 zooplankton predator. The zooplankton model (Mitra 2006) has been validated against
231 various data sets, and used previously in the type of simulation deployed here (e.g., Mitra *et*
232 *al.* 2007). The zooplankton parameters were set for a micro-zooplanktonic predator as per
233 details in Mitra (2006); values for the maximum ingestion rate (G_{\max}) and the half-saturation
234 constant for ingestion (K_{pred}) are in table 2. The stoichiometric (C:N:P) basis of the trophic
235 interactions described in the predator-prey simulations have a well known, firm, basis in the
236 literature (Sterner & Elser 2002; Grover 2003; Mitra & Flynn 2005). In essence, an increasing
237 disparity between the C:N:P of the microalgal prey and its zooplankton predator has a
238 deleterious impact, adversely affecting growth of the predator and nutrient (ammonium and
239 phosphate) regeneration.

240 Predator-prey simulations were run in a dynamic system describing a mixed layer
241 depth of 10m, with mixing into and out of the mixed layer at 0.05 d^{-1} , and assuming an initial
242 (and sub-mixed layer) nitrate concentration of $10 \mu\text{M}$. Phosphate was supplied at a mole ratio
243 (nutrient N:P) of either 16 or 64, equating to pristine or eutrophically skewed conditions,
244 respectively. Light at the surface was described as for the culture simulations (Section 2.3),
245 however as the simulation developed the depth-integrated light field available to the
246 microalgae decreased rapidly from an average daylight value of ca. $500 \mu\text{mol photons m}^{-2} \text{ s}^{-1}$
247 at the start of the simulation to below $50 \mu\text{mol photons m}^{-2} \text{ s}^{-1}$ at the peak of the bloom.

248 The predator-prey simulations presented here assume no genetic modification of algal
249 fatty acid composition or of other factors that may adversely affect palatability to the predator
250 (Mitra & Flynn 2005). As such, the results from the predator-prey simulations represent best-
251 case scenarios. Genetic modification of the fatty acid content (profile) has already been
252 explored (James *et al.* 2011; Radakovits *et al.* 2011; Lei *et al.* 2012), though the implications
253 of this on palatability to grazers await clarification.

254

255

256 3. RESULTS

257 Additional results are presented in supplementary material available online (e-
258 appendix) and are referenced as figure S1, S2 etc.

259

260 3.1 Optimization of biofuels production

261 The key results from our analyses of GM optimisation of production are summarised
262 in figure 1; other results are given in the supplementary e-appendix (figures S1-S4). For
263 optimising biofuels production, the most important phenotypic physiological features are
264 maximising growth rate (μ_{\max} ; figure 1a), minimising the maximum photopigment content
265 (ChlC_{\max} ; figure 1b), and maximising the efficiency of the light capture process (α^{Chl} ;
266 figure 1c). There are important, yet typically overlooked, differences between optimising
267 production of microalgal biomass versus production of biofuels. Biofuels content (excess-C
268 content) relates inversely to the N-limited status of the cells (equation 1), thus for maximum
269 biofuels production (figure 1a) cells need to be grown under N-limiting conditions at their
270 lowest relative growth rate (μ/μ_{\max}). Therefore, although microalgae are typically grown
271 commercially in systems operating at low dilution rates (and hence low μ), highest biofuels
272 production will be realised through the use of cells with the highest potential for growth (high
273 μ_{\max}). Furthermore, avoiding light limitation is an essential prerequisite in the optimisation of
274 biofuels production, thus limiting self-shading (by lowering ChlC_{\max}) and maximising light-
275 conversion to biomass (raising α^{Chl}) are critically important features. The form of the plots in
276 figure 1a reflect this interplay between nutrient status, pigmentation and thus self shading, and
277 production. Simulations using high nutrient loads (e.g., $5 \times f/2$) yielded low biofuels
278 production, because the simulated organisms never exhausted the available nutrients (not
279 shown).

280 Lowering the minimum cellular content of nitrogen (NC_0 , figure 1d) and of
281 phosphorus (PC_0 , figure S1a), and enhancing the efficiency of the use of cellular N and P
282 (KQP and KQN, figures S1b, S1c), give relatively minor headline enhancements of biofuels
283 production, although there are additional advantages that would likely affect the financial
284 viability of the whole venture (see Discussion). There are also several other physiological
285 characteristics of lesser importance. Minimising respiration rates (figures S2a, S2b) prevents
286 the loss of a proportion of the biofuels-C accumulated during day to support night-time
287 respiration. Decreasing the rate of photoacclimation, the process by which microalgae
288 increase their pigment content in response to light limitation (including at night time), is also
289 useful (figure S2c), as it slows the self-shading event that decreases the accumulation of

290 excess-C. Lowering the C:N ratio of core nitrogenous components and of the amount of C
291 allocated to cell structure also have potential to slightly enhance biofuels production (figure
292 S3).

293 In reality, no GM changes will occur alone. In figure S4 we show the combined effects
294 of changing factors associated with photosynthesis, N or P physiology. Of these, the changed
295 photosynthetic configurations (figure S4a) are the most powerful, with scope even when used
296 alone to raise production by ca. 3 fold. While productivity gains through enhancing the
297 efficiency of the use of N and P (KQN and KQP) appear relatively minor, cost effectiveness
298 in fertilizer usage will improve.

299

300 **3.2 Predator-prey interactions**

301 Having explored the optimal configuration of microalgae for biofuels production, we
302 now consider whether zooplankton grazing could likely contain the escape of such an
303 organism to nature. Here, the growth conditions are very different, with a large optical depth
304 and low nutrient concentrations. We compared the predator-prey interactions between a
305 zooplanktonic predator (Mitra 2006) predating either a naturally configured (non-GM)
306 microalgal prey or a GM biofuels-optimised microalgal prey. For this, we used only a mid-
307 range GM configuration (table 2, Cf. table 1), but even this shows greatly improved biomass
308 and biofuels production capabilities over the non-GM form (figure S5).

309 Our simulations with the non-GM microalga show the expected importance of
310 elemental stoichiometry (C:N:P) in the predator-prey interaction (figure 2), with algal prey of
311 a high C content (high C:N and/or C:P) being of poor nutritional value. The adverse impact of
312 food quality on zooplankton becomes particularly apparent under P-limitation, i.e., under
313 nutrient-supply conditions with skewed N:P ratios typical of eutrophication (figure 2b). The
314 combination of characteristics in the GM biofuels-optimised microalgae gives a clear
315 enhanced potential for such organisms forming a poorly grazed bloom (figure 2). Firstly, this
316 status is attained through more rapid growth, forming higher population densities than given
317 by the comparative non-GM configuration for a given nutrient load, and thus out-stripping
318 zooplankton predation control. Secondly, there is the ability of the GM microalgae to become
319 more C-rich, exacerbating the already damaging skewed stoichiometry in nutrient-limited
320 microalgae, and hence disrupting the trophic dynamics which may otherwise restrain net
321 microalgal growth. Of the individual GM characteristics considered, those for μ_{\max} , ChlC_{\max} ,
322 and especially PC_0 appear most important as potentially damaging characteristics in such an
323 organism released to nature (figures S6-S11). We also explored other combinations of

324 physical-nutrient descriptions (shallower versus deeper, with different nutrient loads),
325 obtaining broadly similar responses, with the GM biofuels-optimised microalgae always
326 displaying an enhanced scope for forming large poorly grazed blooms (not shown).

327

328 **4. DISCUSSION**

329 **4.1 The advantages of deployment of GM microalgae for biofuels production**

330 Our analysis shows a potential for an increase in biofuels production from microalgae
331 by perhaps five fold through modifying phenotypic characteristics. The exact gain will depend
332 on many factors, but a gain of four fold is attainable by deploying the GM versus the non-GM
333 configurations described in table 2, and these are not the extreme GM configurations tested
334 (table 1). The optimal configuration for a biofuels producing microalgae is to have (in
335 approximate order of importance) a high μ_{\max} , high α^{Chl} , low ChlC_{\max} , low minimum P:C and
336 N:C contents, low photoacclimation and dark respiration rates, and high efficiency in the use
337 of P and N. Collectively these features endow the organism with an ability to grow rapidly in
338 low light conditions, use relatively little nutrients, more rapidly attain higher biomass and
339 biofuels levels than normal, and be capable of attaining more extreme C:N and C:P levels, and
340 hence contain more biofuels potential per unit of biomass. While such guidelines would help
341 focus selection of wild-type algal strains, most likely a real enhancement would require
342 specific attention to genetic modification of these phenotypic facets.

343 One feature, high maximum growth rates (μ_{\max}), may appear surprising as a preferred
344 characteristic given that continuous culture (chemostat-style) systems are typically run at low
345 dilution rates, thus minimising consumption of fresh media. The reason for the importance of
346 a high μ_{\max} is because the production of excess C-rich metabolites that may act as stock for
347 biofuels is driven primarily as a stress response to an excess supply of fixed C over supply of
348 nutrients (notably of N). The greater the disparity between the growth rate (μ) and the
349 potential maximum rate (μ_{\max}), the greater the potential for the accumulation of excess-C; this
350 is a function of the well documented relationship between cellular nutrient quotas and μ
351 (Droop 1968, Flynn 2008). However, prolonged growth at low dilution rates (forcing low
352 growth rates) selects for a decrease in μ_{\max} (Droop 1974), presumably as the metabolism of
353 the organisms downshifts through adaptation, thus minimising metabolic stress (Flynn 2009).
354 This likely presents a challenge for the deployment of microalgae selected or genetically
355 modified to achieve high growth rates, as with time the characteristic is likely to be lost
356 (selected against) during growth at enforced low growth rates.

357 Lowering the minimum cellular content of nitrogen (NC_0 , figure 1d) and phosphorus
358 (PC_0 , figure S1a), and enhancing the efficiency of the use of cellular N and P (KQP and
359 KQN, figures S1b, S1c) appears to provide only minor enhancements of biofuels production.
360 However, there are important operational and other commercial benefits of such
361 configurations through minimising nutrient usage (Clarens *et al.* 2010; Greenwell *et al.* 2010).
362 This is especially important for P as it is projected that readily available, relatively cheap,
363 sources of phosphate will become increasingly limiting over the coming decades (Cordell *et al.*
364 2009). Additionally, the lower the P-demand by the microalgae the more likely it is that
365 cells become N and not P limited when grown at a given nutrient N:P; this aids development
366 of high C:N (Flynn 2008a, 2008b) and hence further enhances the potential for biofuels
367 production.

368 Some of the features identified in our analysis would be easier to engineer than others
369 and, critically, some will be more stable to mutation, selection and competition pressures.
370 Already the photosystem antennae size has been subjected to GM (Beckmann *et al.* 2009;
371 Melis 2009); this has some leverage on decreasing $ChlC_{max}$, and enhances production (figure
372 1b). While possession of a low $ChlC_{max}$ is likely not a stable trait (Flynn *et al.* 2010),
373 minimising the use of nutrients is likely to be stable as it confers well documented advantages
374 (Liu *et al.* 2001). Modifications of features influencing fundamental aspects of the generation
375 of photoreductant, affecting the value of α^{Chl} , are likely to give stable traits though they will
376 be far more challenging (perhaps currently impossible) to achieve.

377 A feature of the biofuels value of the microalgae that we do not explore in our analysis
378 is the biochemical differentiation of the excess C between starch and lipid/ fatty acids. The
379 nature of this surplus-C is important from a physiological perspective (as the synthesis of lipid
380 is expensive relative to that of carbohydrate (Williams & Laurens 2010)), as well as from a
381 biofuels perspective (Greenwell *et al.* 2010). While it is quite likely that attempts will
382 continue to be made to genetically modify the biochemistry of this material (Beer *et al.* 2009;
383 Li *et al.* 2010; Radakovits *et al.* 2010), and indeed other facets of the organism (such as
384 features affecting the ease of harvesting, tolerance to temperature and salinity etc.), the
385 characteristics that we consider represent primary features affecting microalgal growth and
386 costs in terms of nutrient demand and production. The issue of such biochemical modification
387 of lipid and/or carbohydrate does not affect the central message of the research presented
388 here, not least because it does not alter the key features of the stoichiometric-inspired
389 predator-prey interactions that we consider. Indeed, what will exacerbate the deterioration of
390 the predator-prey interaction (increasingly the likelihood of a HAB) is a change in the quality

391 of the fatty acid such that it no longer contains metabolically important PUFA (Dalsgaard *et*
392 *al.* 2003) and/or it contains a higher proportion of biofuels-desirable short chain saturate fatty
393 acids (James *et al.* 2011; Radakovits *et al.* 2011), or even includes exotic fatty acids that are
394 indigestible, unpalatable, or toxic.

395

396 **4.2 Potential environmental risks posed by biofuels-optimized GM-microalgae**

397 For microalgae to provide any significant contribution to biofuels production they will
398 need to be grown over vast areas. It is most unlikely that all of that growth would be under
399 cover, and even then it is unrealistic to expect that leakage or spillage of some proportion of
400 the many thousands of cubic metres of culture that would be harvested per week would never
401 occur. In all reality then, we need to consider the impact of such a leakage to the environment.

402 The features of a biofuels-optimised microalga, and their likely genetic stability, have
403 important implications for ecology when such an organism enters the natural environment.
404 Previously we reported that during algal-algal competition a microalga with a lower ChlC_{max} ,
405 while being superior as a clonal crop organism, would be at considerable selective
406 disadvantage and would likely be eradicated in the natural environment (Flynn *et al.* 2010).
407 However, as we warned in that previous work, this assumes that the control of growth by
408 predators is equally distributed and does not discriminate in favour of the low ChlC_{max}
409 configured organism. Predator-prey systems are sensitive to such discriminations, and
410 microalgae that appear outwardly poorly competitive with other microalgae can still grow to
411 form dominant ungrazed blooms through such mechanisms (Mitra & Flynn 2006). The
412 configuration of biofuels-optimised microalgae that we identify here is, other than the issue of
413 ChlC_{max} , highly competitive in comparison with the default configuration. If such an
414 organism became the dominant primary producer it would inevitably form dense blooms, for
415 that is what it is designed for, albeit in ponds or other culture systems.

416 While the ability to grow rapidly under low light is important for competition with
417 other phototrophs, of the factors we explored, it is the extreme C:N and C:P ratios in biofuels-
418 optimized micoroalgae that create the greatest risk to trophic dynamics. Such extreme ratios,
419 and the ability to continue to grow rapidly with high fatty acid and/or starch content creates a
420 severe nutritional stoichiometric challenge for zooplankton growth (Grover 2003; Mitra &
421 Flynn 2005, 2006; Mitra 2006). This limits predation upon the simulated GM organism,
422 especially under P-limitation (figures 2b, S11).

423 While the potential formation of ungrazed HABs indicated in figure 2 simply reflects
424 an imbalance in stoichiometric ecology, characteristics such as fatty acid (Dalsgaard *et al.*

425 2003) and toxin content (Mitra & Flynn 2006; Granéli & Flynn 2006) are of vital ecological
426 importance, affecting zooplankton feeding and growth (Jones & Flynn 2005; Mitra & Flynn
427 2005). Any approach that alters fatty acid profiles in microalgae, especially to the biofuels-
428 preferred shorter, saturated forms (James *et al.* 2011) which have little or no nutritional value
429 to zooplankton, would undoubtedly exacerbate the significance of the already highly
430 damaging stoichiometric imbalance (figure 2). Indeed, even when taken in isolation,
431 modifying microalgae to alter their fatty acid content may be expected to adversely affect
432 predation and increase the potential for them forming ungrazed (perhaps ungrazable) blooms.

433 The implications of changes in palatability and toxin production (as secondary
434 metabolites in nutrient-stress microalgae), which are likely to co-occur with such fatty acid
435 modifications, are well known (Jones & Flynn 2005; Mitra & Flynn 2005, 2006; Granéli &
436 Flynn 2006). In consequence, it is most likely that biofuels-optimised microalgae will be less
437 palatable than assumed in the simulations shown here, giving rise to what Mitra & Flynn
438 (2005) refer to as negative stoichiometric modulation of predation (-ve SMP), a process that
439 effectively shuts down predation very rapidly as C:N rises. The outcomes from such trophic
440 interactions will thus likely be even starker in comparison with the default, wild-type,
441 expectations.

442 One could endeavour to counter the above problems by developing traits that place
443 biofuels microalgae at a distinct competitive disadvantage against their naturally occurring
444 counterparts on escape to natural waters. However, configuring a crop organism in this way
445 would also make it vulnerable to failure against contaminants in a culture system. The fact is
446 that for a microalgae to be a robust commercially successful organism for biofuels production
447 requires that it can outcompete any contaminating microalgae, and also proliferate in the
448 presence of any zooplanktonic (predator) pests. Altering factors such as growth rate or
449 nutrient affinity, so that GM microalgae would only grow well at high nutrient concentrations,
450 would place them at a disadvantage in competition with contaminants in culture systems, and
451 would in any case be selected against even within a clonal crop culture when growing under
452 the nutrient limitation that is required to stimulate biofuels production.

453 One potential solution to this conundrum is to optimise growth of GM biofuels-
454 optimised microalgae in extreme environments, for example with respect to temperature or
455 pH (Spijkerman & Wacker 2011), conditions that would not commonly occur in nature.
456 Whether such growth conditions place an acceptable additional financial and logistic burden
457 on the whole enterprise would need careful consideration, given the massive volumetric scale

458 of biomass production required to provide a significant biofuels production. Such an approach
459 would also itself not be immune from posing risks to the environment.

460 An alternative approach is not to increase biomass production to yield metabolites for
461 biofuels production, but to modify biochemistry to redirect the synthesis of organics away
462 from growth and towards fatty acids, which the cells then release for direct harvesting from
463 the growth medium (Liu *et al.* 2011). This approach could be viewed as having parallels with
464 events that already occur in nature. The production and release of excess polysaccharide from
465 nutrient-stressed microalgae in nature is not uncommon, and causes well documented
466 problems associated with foams and transparent exopolymeric material (Mykkestad 1995;
467 Schilling & Zessner 2011). This released material then promotes the growth of ecosystem
468 disruptive algal blooms through inhibition of grazing, and can also create serious pollution
469 events along coasts (Seuront *et al.*, 2006). While the GM approach to direct extracellular
470 production of material destined for biofuels carries various attraction (notably with respect to
471 harvesting), it may thus also carry with it causes of environmental concern as well.
472 Immobilising the microalgae on some fixed substrate could overcome the risk, assuming that
473 the cells could only grow on the substrate and that challenges of adequate illumination (and
474 hence production) can be overcome amongst the attached microalgae.

475 Finally, it is worth noting that GM terrestrial crops differ greatly from GM microalgae
476 with respect to the potential for environmental damage. While higher plants can be made
477 sterile to limit their spread, by their very nature GM microalgae must be capable of
478 reproduction. Higher plants undergo typically one generation a year; microalgae reproduce
479 daily. Our understanding of the impacts of GM higher plants upon ecology has developed
480 over a few decades, a period of reproductive cycles that GM microalgae would achieve in a
481 week. It will thus take something of the order of a century of higher plant generations to
482 compare with a fraction of one year's growth of microalgal generations. While GM terrestrial
483 plant crops have been deployed without obvious catastrophic impacts on ecology (though
484 certainly not without controversy on this point; Tilman *et al.* 2009), it is not possible to
485 extrapolate an argument that GM microalgae would be similarly benign.

486

487 **5. CONCLUSIONS**

488 There has been much claimed for the potential of algal biofuels to contribute
489 significantly to energy sustainability and security, but detailed analyses indicate that for
490 financial and logistic realisation costs per litre of biofuels need to come down significantly
491 before such a dream can be realised (Clarens *et al.* 2010; Greenwell *et al.* 2010; Williams &

492 Laurens 2010). A major advance may be achieved by attaining a step change in microalgal
493 productivity. Significantly, our previous analysis (Flynn *et al.* 2010) suggests that areal
494 productivity using “typical” microalgae is likely to be little better than that seen under optimal
495 conditions in nature (Sarmiento & Gruber 2006). While in culture ponds the volumetric
496 production is much higher, and hence harvesting and dewatering costs are decreased
497 accordingly, the implication is that areal production using wild-type strains is limited by the
498 total light incident to the culture system and by the underlying physiology of the organisms.
499 That physiology has evolved over millions of years from basic metabolic building blocks with
500 origins to the emergence of life on Earth (Shi *et al.* 2005). To go beyond this (natural
501 maximum) productivity of ca. 4 gC m⁻² d⁻¹ thus requires a change in the physiology of the
502 organisms. It is most likely that this can only be achieved through radical genetic
503 modification, creating organisms that are literally new to nature.

504 Our work indicates a clear potential for GM in the commercial development of
505 microalgal biofuels, with scope for raising production by perhaps half an order of magnitude
506 (figures 1, S5). Coupled with more efficient processing technologies, GM microalgae could
507 make microalgal biofuels a viable and cost-effective option. However, our study also suggests
508 a very real risk that the engineered product could come to represent the perfect harmful algal
509 bloom (HAB) species (figure 2), with all the attendant risks to the environment, to
510 environmental services and human health that HABs present (Glibert *et al.* 2005). This is not
511 to say that all GM approaches will exhibit the same potential risks to nature. However, and
512 accepting that not all of the GM traits may be stable in nature, given the ease with which GM
513 microalgae could be transferred around the planet the potential risk of GM microalgae to
514 nature should not be underestimated. There already exists ample warning of the damage that
515 can be caused from the inadvertent trans-ocean transfers of “exotic” natural HAB species
516 (Hallegraeff 1998), with no evidence that naturally occurring zooplankton can contain the
517 problem. Indeed, disruption to biodiversity by invasive alien species is well known and all too
518 common (e.g., for aquatics, Padilla & Williams 2004). In this capacity, the mass cultivation of
519 any microalga isolated from a source distant to the site of commercial deployment is also a
520 matter of concern.

521 The spread of a GM-microalgae of the type of configuration we identify would be
522 effectively impossible to halt. As GM of factors likely affecting palatability of microalgae is
523 already being conducted in the name of biofuels production (Li *et al.*, 2010; Radakovits *et al.*
524 2011; Lei *et al.* 2012), there is a real risk that the genie is already part way out of the bottle. If
525 GM biofuels-optimised microalgae were to destroy fisheries then a main driver for microalgal

526 biofuels research, the argument that such biofuels production would not compete with
527 production of biomass for food (Chisti 2007; Wijffels & Barbosa 2010), may prove to be
528 totally misplaced. Accordingly, a strong argument can be made for the regulation of GM of
529 microalgal at an international level, because the potential for damage could have global
530 consequences, echoing recent concerns over geoengineering (McNaughton & Owens 2012).
531 Whether, against arguments for sovereign fuel security, regulation could be enforced, is a
532 dilemma that society may soon have to face up to.

533

534 **ACKNOWLEDGEMENTS**

535 This work was part funded by a Fellowship to KJF from The Institute of Advanced Study,
536 Durham University. KJF was also funded by NERC (U.K.) for part of this work. We thank
537 referees to a previous version of this paper for their insightful comments.

538 **REFERENCES**

- 539 Anning, T., Macintyre, H. L., Pratt, S. M., Sammes, P. J., Gibb, S. & Geider, R. J. 2000
540 Photoacclimation in the marine diatom *Skeletonema costatum*. *Limnol. Oceanogr.* **45**,
541 1807–1817.
- 542 Beckmann, J., Lehrb, F., Finazzic, G., Hankamerd, B., Postenb, C., Wobbee, L. & Krusea, O.
543 2009 Improvement of light to biomass conversion by de-regulation of light-harvesting
544 protein translation in *Chlamydomonas reinhardtii*. *J. Biotech.* **142**,70–77.
- 545 Beer, L. L., Boyd, E. S., Peters, J. W. & Posewitz, M. C. 2009 Engineering algae for
546 biohydrogen and biofuel production. *Curr. Opin. Biotech.* **20**, 264-271.
- 547 Courchesne, N. M. D., Parisien, A., Wang, B. & Lan, C. Q. 2009 Enhancement of lipid
548 production using biochemical, genetic and transcription factor engineering approaches
549 *J. Biotech.* **141**, 31–41.
- 550 Chen C.Y., Yeh K.L., Aisyah R., Lee D.J. & Chang J.S. 2011 Cultivation, photobioreactor
551 design and harvesting of microalgae for biodiesel production: A critical review.
552 *Bioresour. Technol.* **102**, 71-81
- 553 Chisti, Y. 2007 Biodiesel from microalgae. *Biotech. Adv.* **25**, 294-306.
- 554 Clarens, A. F., Resurreccion, E. P., White, M. A., & Colosi, L. M. 2010 Environmental life
555 cycle comparison of algae to other bioenergy feedstock, *Environ. Sci. Technol.*, **44**,
556 1813–1819.
- 557 Cordell, D., Drangert, J. & White, S. 2009 The story of phosphorus: Global food security and
558 food for thought. *Global. Environ. Chang.* **19**, 292-305.
- 559 Dalsgaard, J., St. John, M., Kattner, G., Müller-Navarra, D. & Hagen, W. 2003 Fatty acid
560 trophic markers in the pelagic marine environment. *Adv. Mar. Biol.* **46**, 225–340.
561 2003.
- 562 Droop, M. R. 1968 Vitamin B₁₂ and marine ecology. IV. The kinetics of uptake, growth, and
563 inhibition in *Monochrysis lutheri*. *J. Mar. Biol. Assoc. U.K.* **48**, 689–733.
- 564 Droop, M. R. 1974 The nutrient status of algal cells in continuous culture. *J. Mar. Biol. Assoc.*
565 *U.K.* **54**, 825–855.
- 566 Fasham, M. J. R., Flynn, K. J., Pondaven, P., Anderson, T. R. & Boyd, P. W.
567 2006 Development of a robust ecosystem model to predict the role of iron on
568 biogeochemical cycles: a comparison of results for iron-replete and iron-limited areas,
569 and the SOIREE iron-enrichment experiment. *Deep-Sea Res.* **I 53**, 333-366.
- 570 Flynn, K. J. 2001 A mechanistic model for describing dynamic multi-nutrient, light,
571 temperature interactions in phytoplankton. *J. Plankt. Res.* **23**, 977-997.

- 572 Flynn, K. J. 2002 How critical is the critical N:P ratio? *J. Phycol.* **38**, 961-970.
- 573 Flynn, K. J. 2003 Modelling multi-nutrient interactions in phytoplankton; balancing
574 simplicity and realism. *Prog. Oceanogra.* **56**, 249 – 279.
- 575 Flynn, K. J. 2008a Use, abuse, misconceptions and insights from quota models: the Droop
576 cell-quota model 40 years on. *Oceanogra. Mar Biol. Ann. Rev.* **46**, 1-23.
- 577 Flynn, K. J. 2008b The importance of the form of the quota curve and control of non-limiting
578 nutrient transport in phytoplankton models. *J. Plankt. Res* **30**, 423–438.
- 579 Flynn, K. J. 2009 Going for the slow burn: why should possession of a low maximum growth
580 rate be advantageous for microalgae? *Plant Ecol. Diversity* **2**, 179-189.
- 581 Flynn, K. J., Clark, D. R. & Xue, Y. 2008 Modelling the release of dissolved organic matter
582 by phytoplankton. *J. Phycol.* **44**, 1171-1187
- 583 Flynn, K. J., Greenwell, H. C., Lovitt, R. W. & Shields, R. J. 2010 Selection for fitness at the
584 individual or population levels: modeling effects of genetic modifications in
585 microalgae on productivity and environmental safety. *J. Theoret. Biol.* **263**, 269-280.
- 586 Flynn, K. J. & Hipkin, C. R. 1999 Interactions between iron, light, ammonium and nitrate;
587 insights from the construction of a dynamic model of algal physiology. *J. Phycol.* **35**,
588 1171-1190.
- 589 Flynn, K. J., Marshall, H. & Geider, R. J. 2001 A comparison of two N-irradiance models of
590 phytoplankton growth. *Limnol. Oceanogr.* **46**, 1794-1802.
- 591 Geider, R. J. & La Roche, J. 2002 Redfield revisited: Variability of C:N:P in marine
592 microalgae and its biochemical basis. *Eur. J. Phycol.* **37**, 1-17.
- 593 Geider, R. J., Macintyre, H. L. & Kana, T. M. 1998. A dynamic regulatory model of
594 phytoplanktonic acclimation to light, nutrients, and temperature. *Limnol. Oceanogr.*
595 **43**, 679–694.
- 596 Glibert, P. M., Anderson, D. M., Gantner, P., Graneli, E. & Sellner, K. G. 2005 The global
597 complex phenomena of harmful algal blooms. *Oceanography* **18**, 137-147
- 598 Granéli, E. & Flynn, K. J. 2006 Chemical And Physical Factors Influencing Toxin
599 Production. In *Ecology Of Harmful Algae*, eds E. Granéli & J. T. Turner, Ecological
600 Studies, Vol. **189**, 229-241. Springer-Verlag, Berlin.
- 601 Greenwell, H. C., Laurens, L. M. L., Shields, R. J., Lovitt, R. W. & Flynn, K. J. 2010 Placing
602 microalgae on the biofuels priority list: a review of the technological challenges. *J.*
603 *Roy. Soc. Interface* **6**, 703-726.
- 604 Grover, J. P. 2003 The impact of variable stoichiometry on predator-prey interactions: a
605 multinutrient approach. *Am. Nat.* **162**, 29-43.

606 Guillard, R. L. L. & Ryther, J. H. 1962. Studies on marine planktonic diatoms I. *Cyclotella*
607 *nana* Hustedt and *Detonula confervacea* (Cleve). *Grans Can J Microbiol* **8**, 229-239.

608 Hallegraeff, G. M. 1998 Transport of toxic dinoflagellates via ships' ballast water:
609 bioeconomic risk assessment and efficacy of possible ballast water management
610 strategies. *Mar. Ecol. Prog. Ser.*, **168**, 297-309.

611 James, G. O., Hocartb, C. H., Hilliera, W., Chena, H., Kordbacheha, F., Pricea, G. D. &
612 Djordjevica, M. A. 2011 Fatty acid profiling of *Chlamydomonas reinhardtii* under
613 nitrogen deprivation. *Bioresour. Technol.* **102**, 3343-3351.

614 John, E. H. & Flynn, K. J. 2002 Modelling changes in paralytic shellfish toxin content of
615 dinoflagellates in response to nitrogen and phosphorus supply. *Mar. Ecol. Prog. Ser.*
616 **225**, 147-160.

617 Jones, R. H. & Flynn, K. J. 2005 Nutritional status and diet composition affect the value of
618 diatoms as copepod prey. *Science* **307**, 1457-1459.

619 Lei, A., Chen, H., Shen, G., Hu, Z., Chen, L. & Wang, J. 2012 Expression of fatty acid
620 synthesis genes and fatty acid accumulation in *Haematococcus pluvialis* under
621 different stressors. *Biotechnol. Biofuels* **5**,18

622 Li, Y., Han, D., Hu, G., Sommerfeld, M. & Hu, Q. 2010 Inhibition of starch synthesis results
623 in overproduction of lipids in *Chlamydomonas reinhardtii*. *Biotechnol. Bioeng.* **107**,
624 258-268.

625 Liu, H., Laws, E. A., Villareal, T. A. & Buskey, E. J. 2001 Nutrient limited growth of
626 *Aureoumbra lagunensis* (Pelagophyceae), with implications for its capability to
627 outgrow other phytoplankton species in phosphate-limited environments. *J. Phycol.*
628 **37**,500–508.

629 Liu, X., Sheng, J. & Curtiss, R. 2011. Fatty acid production in genetically modified
630 cyanobacteria. *Proc. Natl. Acad. Sci. U. S. A.* **108**, 6899-6904.

631 Macintyre, H. L., Kana, T. M., Anning, T. & Geider, R. J. 2002 Photoacclimation of
632 photosynthesis irradiance response curves and photosynthetic pigments in microalgae
633 and cyanobacteria. *J. Phycol.* **38**, 17-38.

634 McNaughton, P. & R. Owens 2012 Environmental science: Good governance for
635 geoengineering, *Nature* **479**, 293. 2012.

636 Melis, A. 2009 Solar energy conversion efficiencies in photosynthesis: Minimizing the
637 chlorophyll antenna to maximize efficiency. *Plant Sci.* **177**, 272–280.

- 638 Mitra, A. 2006 A multi-nutrient model for the description of stoichiometric modulation of
639 predation (SMP) in micro- and mesozooplankton. *J. Plankt. Res.* **28**,597-611.
- 640 Mitra, A. & Flynn, K. J. 2005 Predator-prey interactions: is “ecological stoichiometry”
641 sufficient when good food goes bad? *J. Plankt. Res.* **27**; 393-399.
- 642 Mitra, A. & Flynn, K. J. 2006 Promotion of harmful algal blooms by zooplankton predatory
643 activity. *Biol. Lett.* **2**, 194-197.
- 644 Mitra, A, Flynn, K. J. & Fasham, M. J. R. 2007 Accounting correctly for grazing dynamics in
645 Nutrient-Phytoplankton-Zooplankton models. *Limnol. Oceanogr.* **52**, 649-661.
- 646 Myklestad, S. M. (1995) Release of extracellular products by phytoplankton with special
647 emphasis on polysaccharides. *Sci. Total. Environ.* **165**, 155-164.
- 648 Padilla, D. K. & Williams, S. L. 2004. Beyond ballast water: aquarium and ornamental trades
649 as sources of invasive species in aquatic ecosystems. *Front. Ecol. Environ.* **2**, 131-138.
- 650 Radakovits, M, Eduafo, P. M. & Posewitz, M. C. 2011 Genetic engineering of fatty acid chain
651 length in *Phaeodactylum tricorutum*. *Metabolic Engineering* **13**, 89–95
- 652 Radakovits, R. Jinkerson, R. E., Darzins, A. & Posewitz, M. C. 2010 Genetic engineering of
653 algae for enhanced biofuel production. *Eukaryotic cell* **9**, 486-501.
- 654 Sarmineto, J. L. & Gruber, N. 2006 *Ocean Biogeochemical Dynamics*. Princeton University
655 Press, New Jersey, USA.
- 656 Schilling, K. & Zessner, M. 2011 Foam in the aquatic environment. *Water Res.* **45**, 4355-
657 4366.
- 658 Seuront, L., Vincent, D. & Mitchell, J. G. 2006 Biologically induced modification of seawater
659 viscosity in the Eastern English Channel during a *Phaeocystis globosa* spring bloom.
660 *J. Mar. Sys.* **61**, 118–133
- 661 Shi, T., Bibby, T. S., Jiang, L., Irwin, A. J. & Falkowski, P.G. 2005. Protein interactions limit
662 the rate of evolution of photosynthetic genes in cyanobacteria. *Mol. Biol. Evol.* **22**,
663 2179–2189.
- 664 Shirvani, T., Yan, X., Inderwildi, O. R., Edwards, P. . & King, D. A. 2011 Life cycle energy
665 and greenhouse gas analysis for algae-derived biodiesel. *Energy Environ. Sci.* **4**, 3773-
666 3778
- 667 Smith, B., Greenwell, H. C. & Whiting, A. 2009 Catalytic upgrading of tri-glycerides and
668 fatty acids to transport biofuels. *Energy Environ. Sci.* **2**, 262-271.

669 Spijkerman, E. & Wacker, A. 2011 Interactions between P-limitation and different C
670 conditions on the fatty acid composition of an extremophile microalga. *Extremophiles*
671 **15**, 597-609.

672 Sterner, R. W. & Elser, J. J. 2002 *Ecological Stoichiometry: the Biology of Elements from*
673 *Molecules to the Biosphere*. Princeton University Press, Princeton, NJ, U.S.A.

674 Tilman, D., Socolow, R., Foley, J. A., Hill, J., Larson, E., Lynd, L., Pacala, S., Reilly, J.,
675 Searchinger, T., Somerville, C. & Williams, R. 2009 Beneficial biofuels - the food,
676 energy, and environment trilemma. *Science* **325**, 270-271.

677 Wijffels, R. H. & Barbosa, M. J. 2010 An outlook on microalgal biofuels. *Science* **329**, 796-
678 799.

679 Williams, P. J. le-B. & Laurens, L. M. L. 2010 Microalgae as biodiesel & biomass feedstocks:
680 Review & analysis of the biochemistry, energetics & economics *Energy Environ. Sci.*,
681 **3**, 554–590.

682

683

684 LEGENDS

685

686 **Table 1**

687 Parameter values for the base non-GM model and ranges explored for the GM counterparts.

688 Values are also given for the physico-chemical culture system; also see text. The nutrient

689 regime equates to that of the classic f/2 medium (Guillard & Ryther 1962) containing 882 μ M

690 N and 36.2 μ M P

691

692 **Table 2**

693 Parameters for model runs shown in figure 2 and as indicated in figure legends for figures S5-

694 S11. See Methods, and table 1 for further information.

695

696 **Figure 1.** Biomass and biofuels areal production. Variation of areal production of biomass

697 (left hand plots) and biofuels (middle plots) against dilution rate (=growth rate, μ) for

698 different physiological characteristics under chemostat-style steady-state conditions. The right

699 hand plots show the percentage of biomass as biofuels; note the different axes directions. Part

700 (a), maximum growth rate (μ_{\max}). Part (b), maximum chlorophyll content (ChlC_{\max}). Part (c),

701 overall phenotypic efficiency of the photochemistry (α^{Chl} , given here with units of

702 ($\text{mgC } \mu\text{mol}^{-1} \text{ photon}$) ($\text{m}^2\text{g}^{-1} \text{ chl.a}$)). Part (d), minimum (subsistence) quota for N (NC_0 , N:C).

703 Note that at high dilution rates biofuels production falls as the microalgae become N-

704 sufficient.

705

706 **Figure 2.** Predator-prey simulations. Simulated interaction between a microalgal prey (Algae)

707 and its zooplanktonic predator (Zoo). Simulations were run with the microalga configured to

708 represent a non-GM (thin line) or a biofuels optimised GM strain (thick line); see table 2. In

709 panel (a) the mole nutrient ratio is N:P = 16 representing pristine water bodies. In panel (b)

710 N:P = 64, representing the skewed nutrient content seen in eutrophic coastal waters. Temporal

711 development of the interaction would depend on initial conditions. Plots show development of

712 the algal and zooplankton biomass, and changes in the algal N:C and P:C ratios. Decreases in

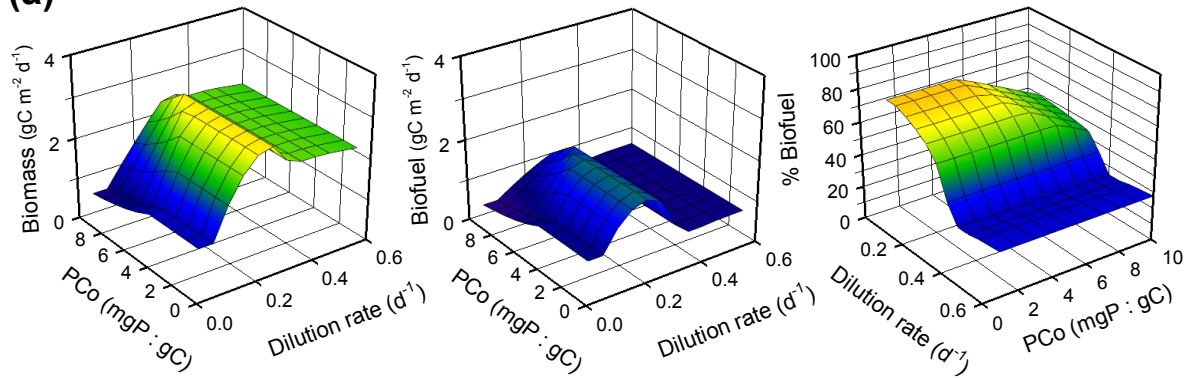
713 algal N:C and P:C indicate changes in nutrient stress (through exhaustion of external nutrient

714 supply).

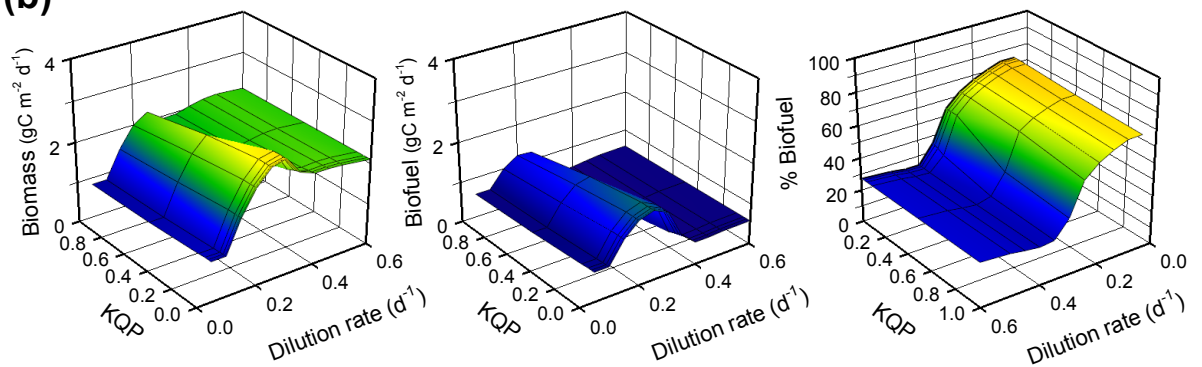
715

SUPPLEMENTARY FIGURES

(a)



(b)



(c)

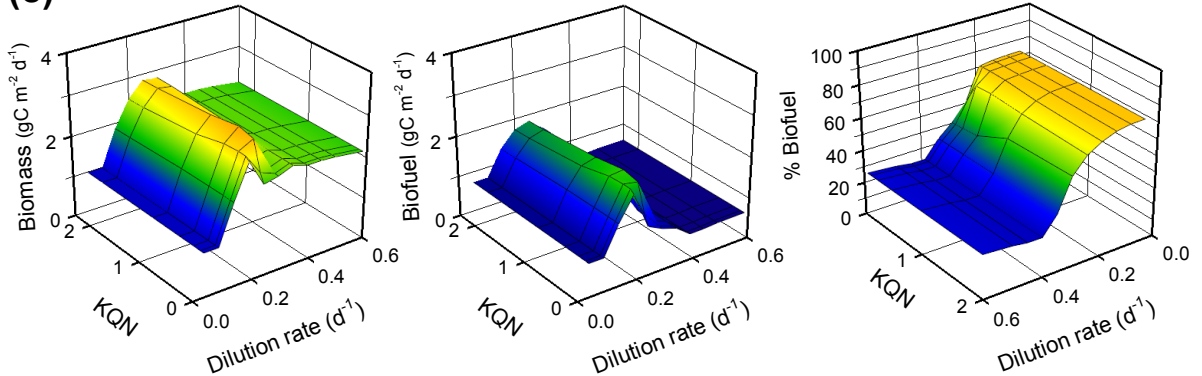


Figure S1. Variation of biomass (left hand plots) and biofuels (middle plots) areal production against dilution rate (=growth rate, μ) for different physiological characteristics. The right hand plots show the percentage of biomass as biofuels; note the different axes directions. Part (a), the minimum (subsistence) quota for P (PC_0); see figure 1d for the N subsistence quota. Part (b), constant describing the efficiency of P utilisation during growth (KQP , low values are more efficient). Part (c), constant describing the efficiency of N utilisation during growth (KQN , low values are more efficient). Note that at high dilution rates, biofuels production can fall as the microalgae become N-sufficient.

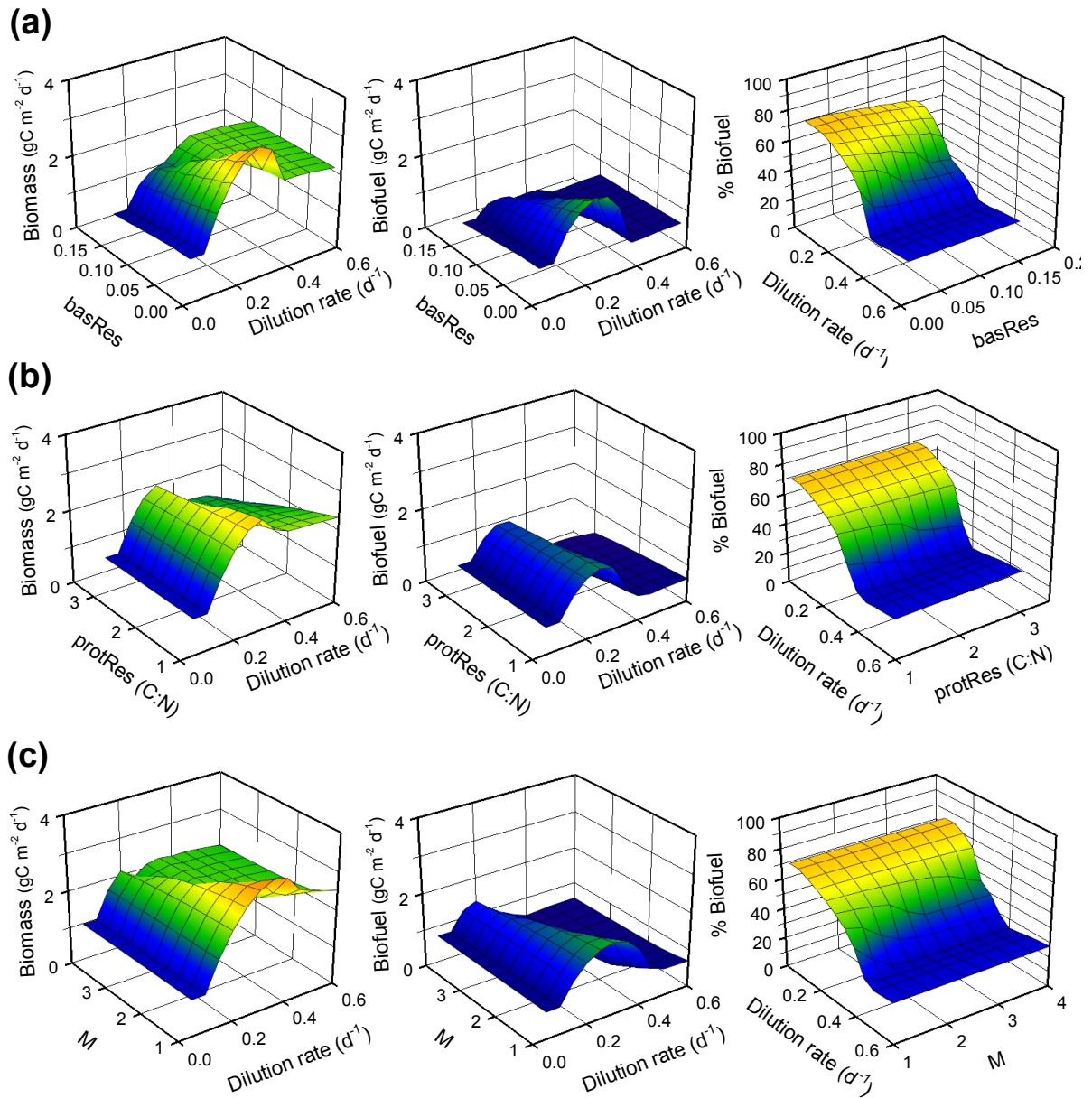


Figure S2. Variation of biomass (left hand plots) and biofuels (middle plots) areal production against dilution rate (=growth rate, μ) for different physiological characteristics. The right hand plots show the percentage of biomass as biofuels; note the different axes directions. Part (a), basal respiration rate (basRes, as a percentage of maximum growth rate). Part (b), metabolic respiration rate for protein synthesis (protRes). Part (c), index for the rate of photoacclimation (M). Note that at high dilution rates biofuels production can fall as the microalgae become N-sufficient.

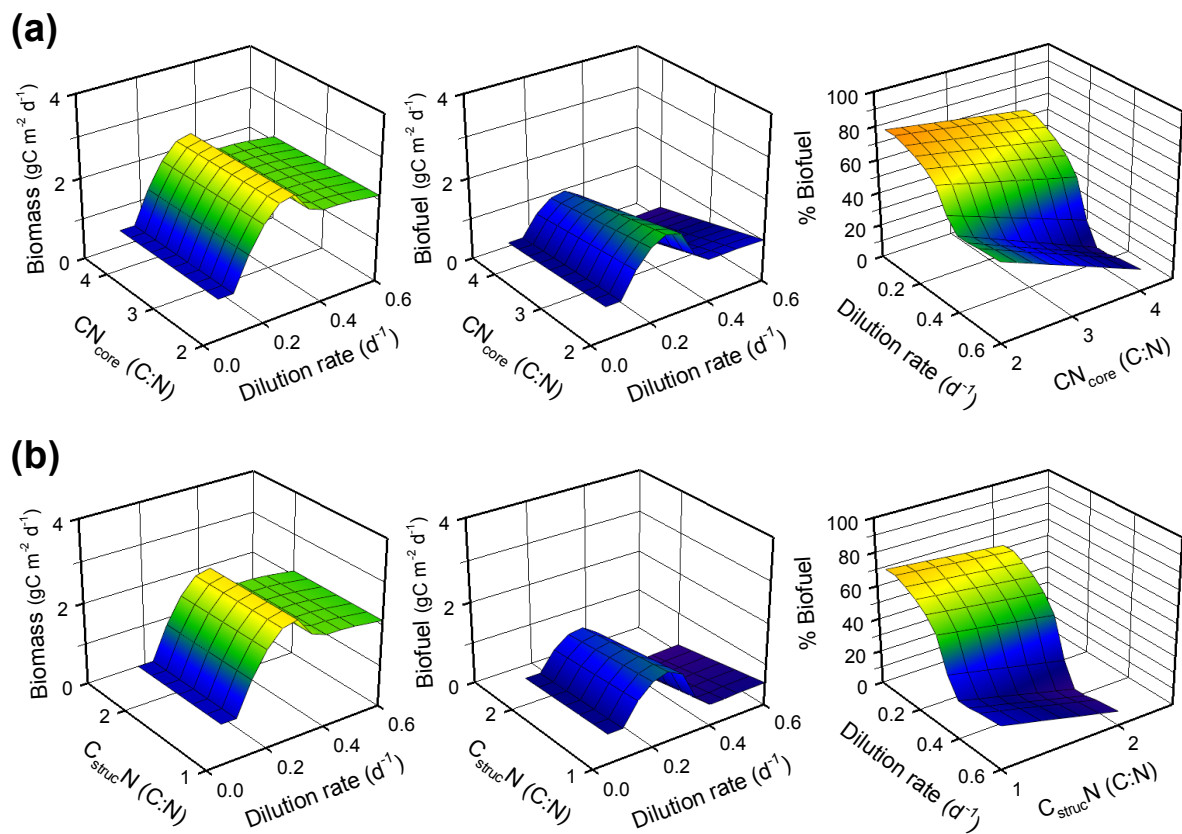


Figure S3. Variation of biomass (left hand plots) and biofuels (middle plots) areal production against dilution rate (=growth rate, μ) for different physiological characteristics. The right hand plots show the percentage of biomass as biofuels; note the different axes directions. Part (a), the C:N ratio for the core nitrogenous material (CN_{core} ; protein + DNA + RNA). Part (b), the C allocation to the non-nitrogenous structural material (cell walls, membranes) as a ratio of the nitrogenous components ($C_{struc}N$). Note that at high dilution rates biofuels production can fall as the microalgae become N-sufficient.

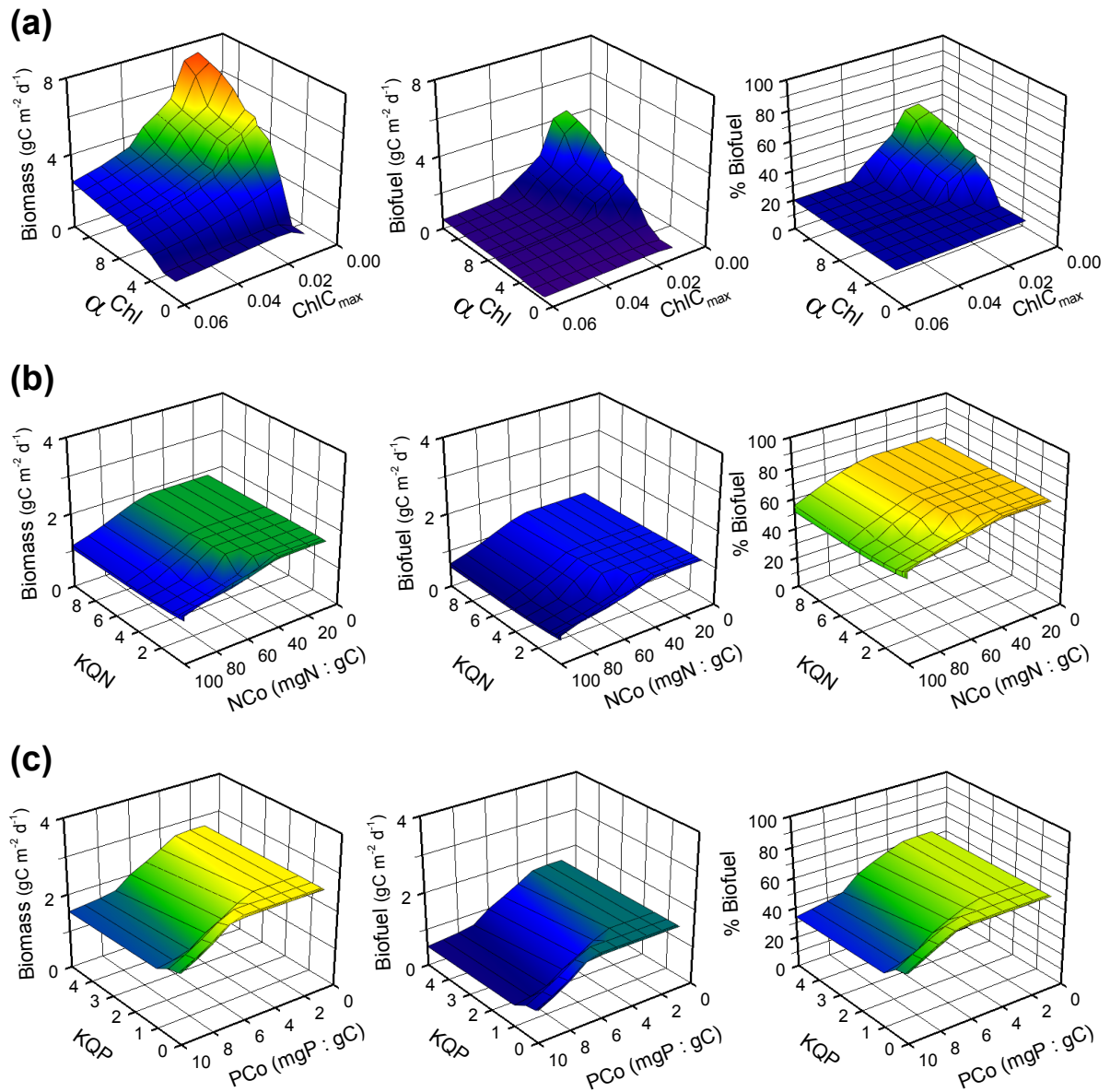


Figure S4. Variation of biomass (left hand plots) and biofuels (middle plots) areal production as a function of different pairs of physiological characteristics. The right hand plots show the percentage of biomass as biofuels. The dilution rate (= growth rate, μ) was fixed at 0.2 d^{-1} . Part (a), maximum Chl:C ($Chl:C_{max}$) versus the overall phenotypic efficiency of the photochemistry (α^{Chl} , given here with units of $(\text{mgC } \mu\text{mol}^{-1} \text{ photon}) \cdot (\text{m}^2\text{g}^{-1} \text{ chl.a})$). Part (b), minimum (subsistence) quota for N (NC_0) versus the constant parameter describing efficiency of N utilisation during growth (KQN , low values are more efficient). Part (c), minimum (subsistence) quota for P (PC_0) versus the constant describing the efficiency of N utilisation during growth (KQP , low values are more efficient).

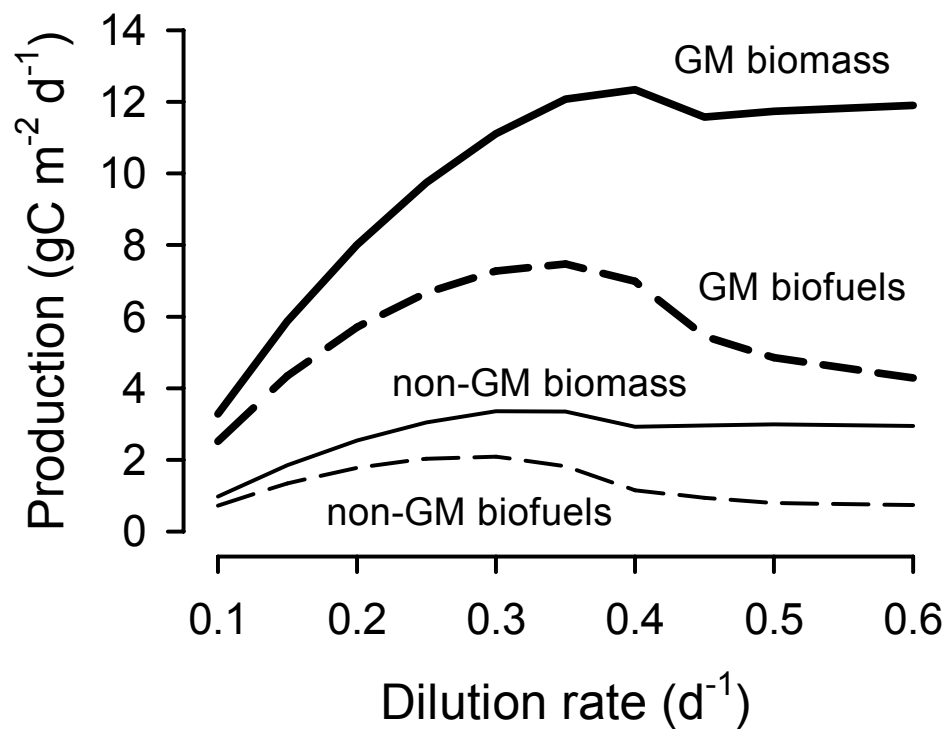


Figure S5. Steady-state rates of production using microalgae configured as non-GM or GM configurations as described in table 2. Maximum rates of production were achieved with nutrient concentrations of $f/2$ for the non-GM algae, but with $3 \times f/2$ for the GM algae; the latter configuration enables growth to higher densities because the pigmentation level is restricted (i.e., ChlC_{max} is lower).

GM μ_{\max}

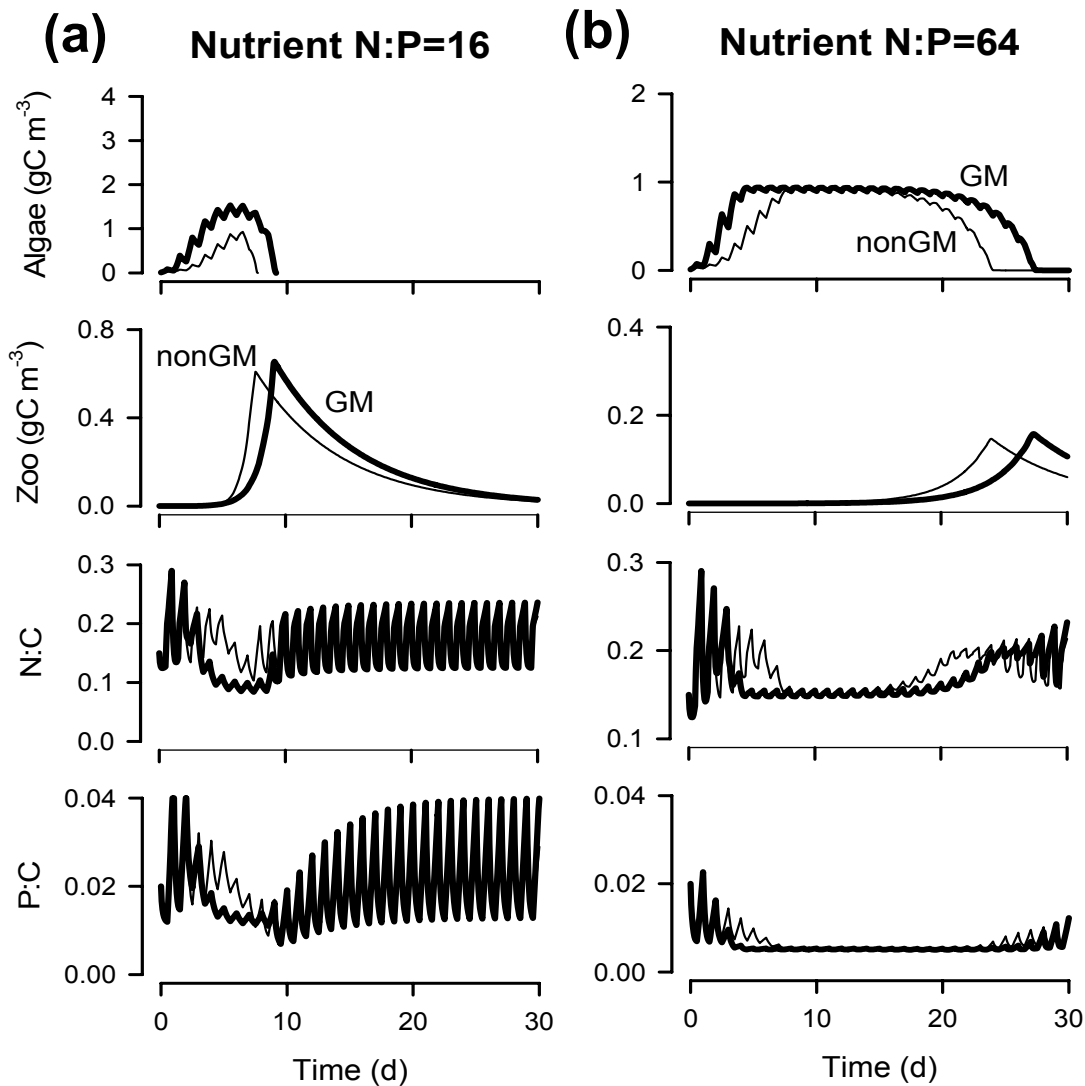


Figure S6. Simulated interaction between a microalga and its zooplanktonic predator. Simulations were run with the microalga configured to represent a non-GM or a GM strain with elevated μ_{\max} . See table 2 for further details. In panel (a) the mole nutrient ratio is N:P 16, as expected in pristine water bodies. In panel (b) N:P is 64, representing the skewed nutrient content seen in eutrophic coastal waters. The temporal development of the interaction would depend on initial conditions. Plots show development of the algal and zooplankton biomass, and changes in the algal N:C and P:C ratios. Decreases in N:C and P:C indicate changes in nutrient stress (through exhaustion of external nutrient supply).

GM ChIC_{max}

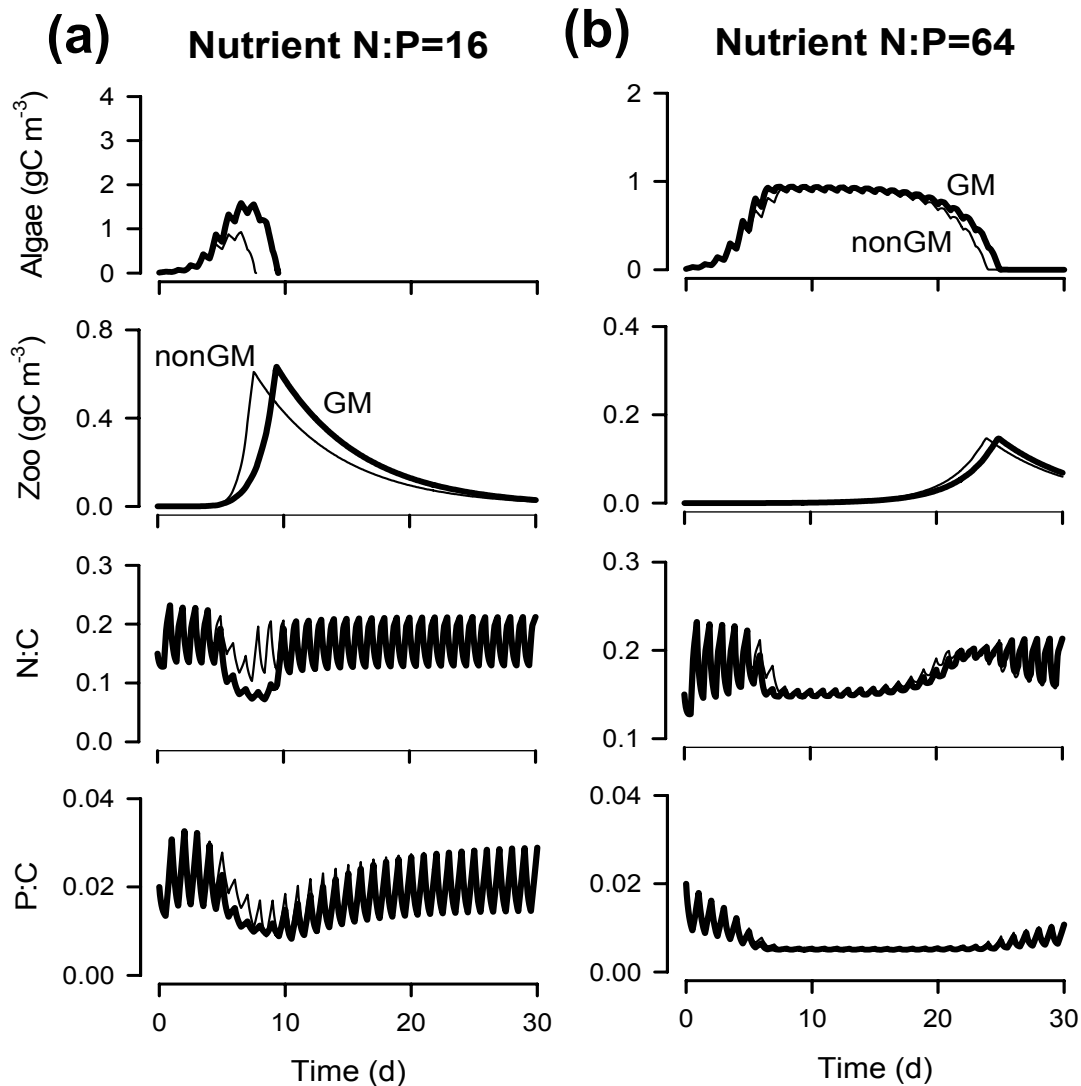


Figure S7. Simulated interaction between a microalga and its zooplanktonic predator. Simulations were run with the microalga configured to represent a non-GM or a GM strain with a depressed ChIC_{max}. See table 2 for further details. In panel (a) the mole nutrient ratio is N:P 16, as expected in pristine water bodies. In panel (b) N:P is 64, representing the skewed nutrient content seen in eutrophic coastal waters. The temporal development of the interaction would depend on initial conditions. Plots show development of the algal and zooplankton biomass, and changes in the algal N:C and P:C ratios. Decreases in N:C and P:C indicate changes in nutrient stress (through exhaustion of external nutrient supply).

GM α^{Chl}

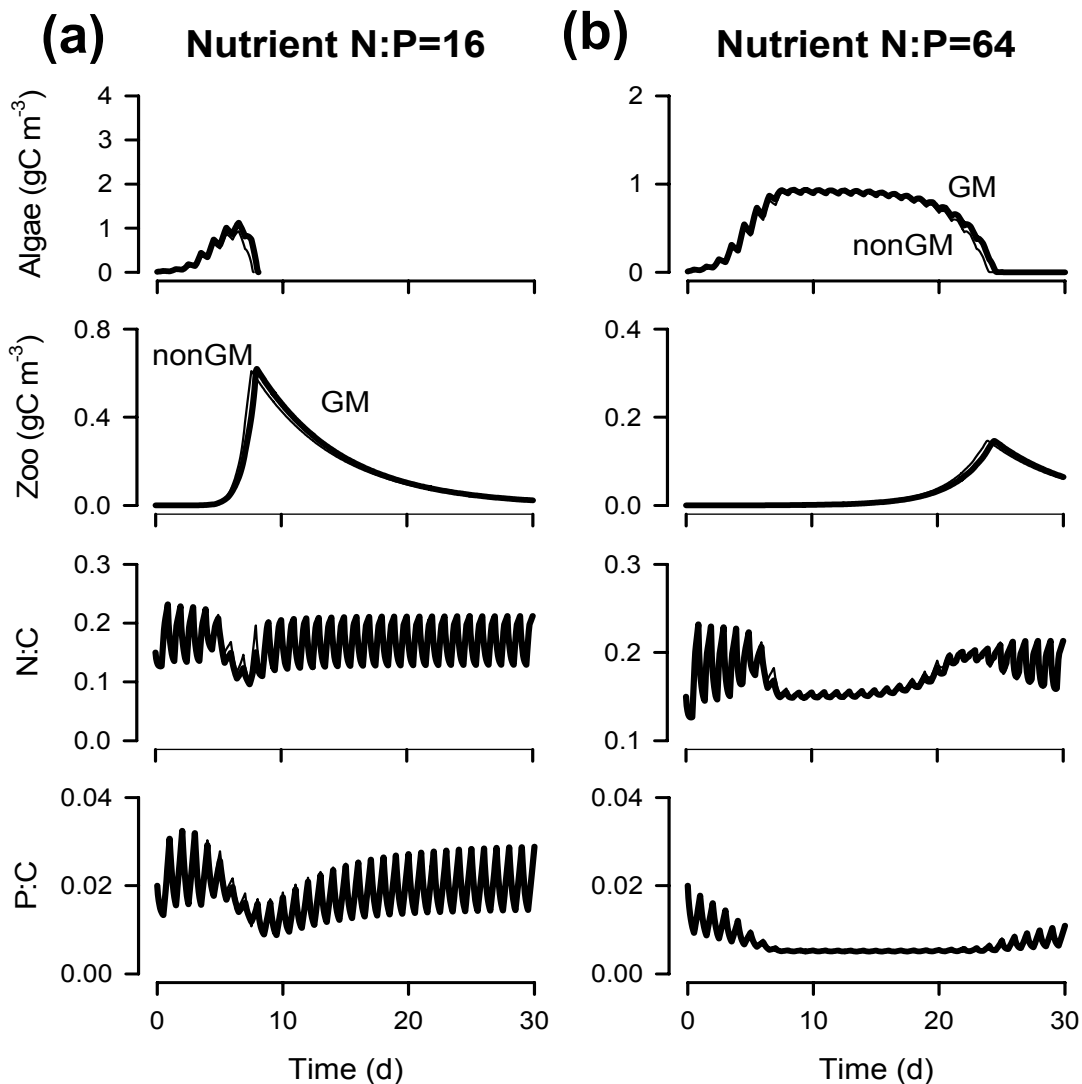


Figure S8. Simulated interaction between a microalga and its zooplanktonic predator. Simulations were run with the microalga configured to represent a non-GM or a GM strain with elevated α^{Chl} . See table 2 for further details. In panel (a) the mole nutrient ratio is N:P 16, as expected in pristine water bodies. In panel (b) N:P is 64, representing the skewed nutrient content seen in eutrophic coastal waters. The temporal development of the interaction would depend on initial conditions. Plots show development of the algal and zooplankton biomass, and changes in the algal N:C and P:C ratios. There are very few points of difference between the non-GM and GM configurations. Decreases in N:C and P:C indicate changes in nutrient stress (through exhaustion of external nutrient supply).

GM M

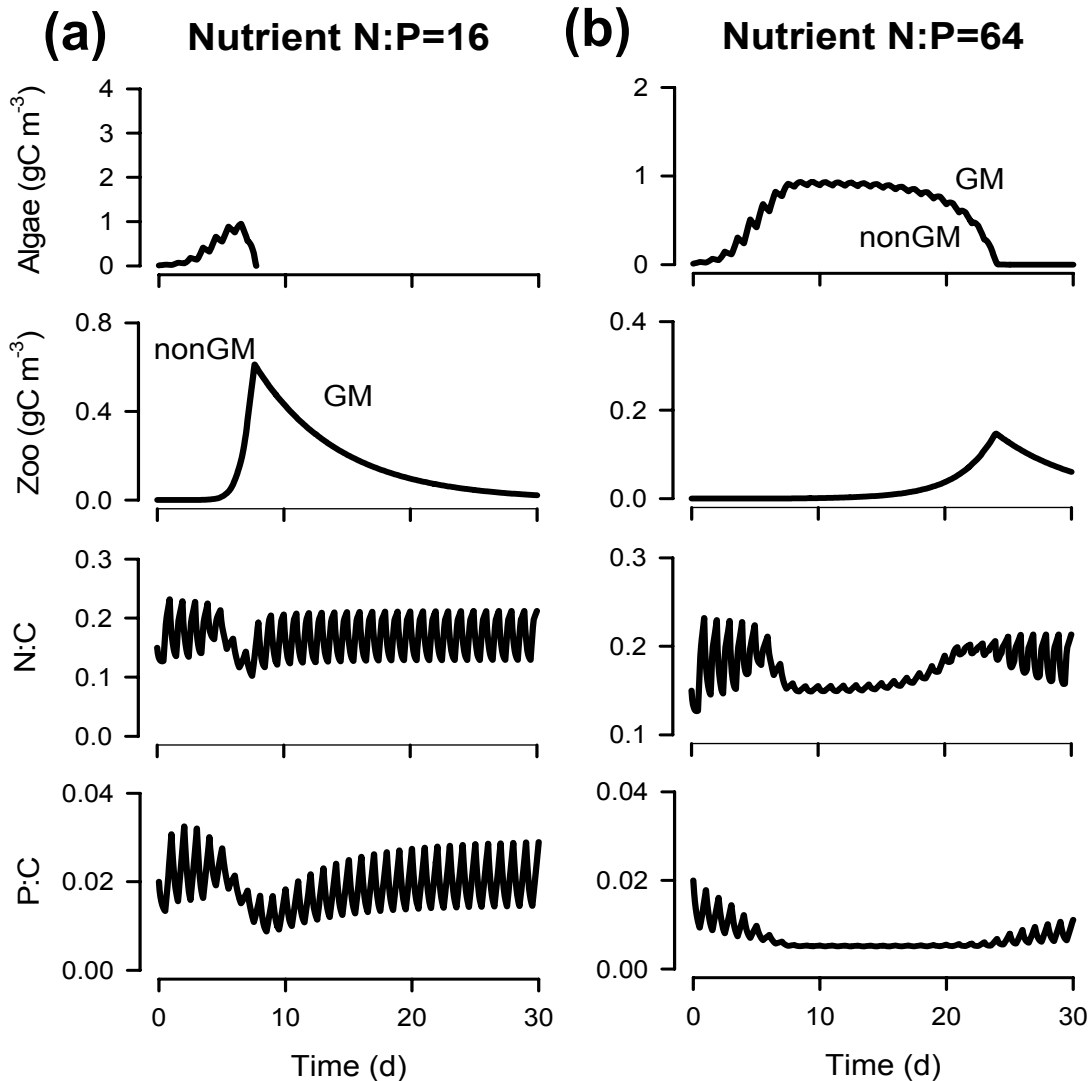


Figure S9. Simulated interaction between a microalga and its zooplanktonic predator. Simulations were run with the microalga configured to represent a non-GM or a GM strain with decreased M . See table 2 for further details. In panel (a) the mole nutrient ratio is N:P 16, as expected in pristine water bodies. In panel (b) N:P is 64, representing the skewed nutrient content seen in eutrophic coastal waters. The temporal development of the interaction would depend on initial conditions. Plots show development of the algal and zooplankton biomass, and changes in the algal N:C and P:C ratios. Decreases in N:C and P:C indicate changes in nutrient stress (through exhaustion of external nutrient supply). There are essentially no points of difference between the non-GM and GM configurations.

GM NC₀

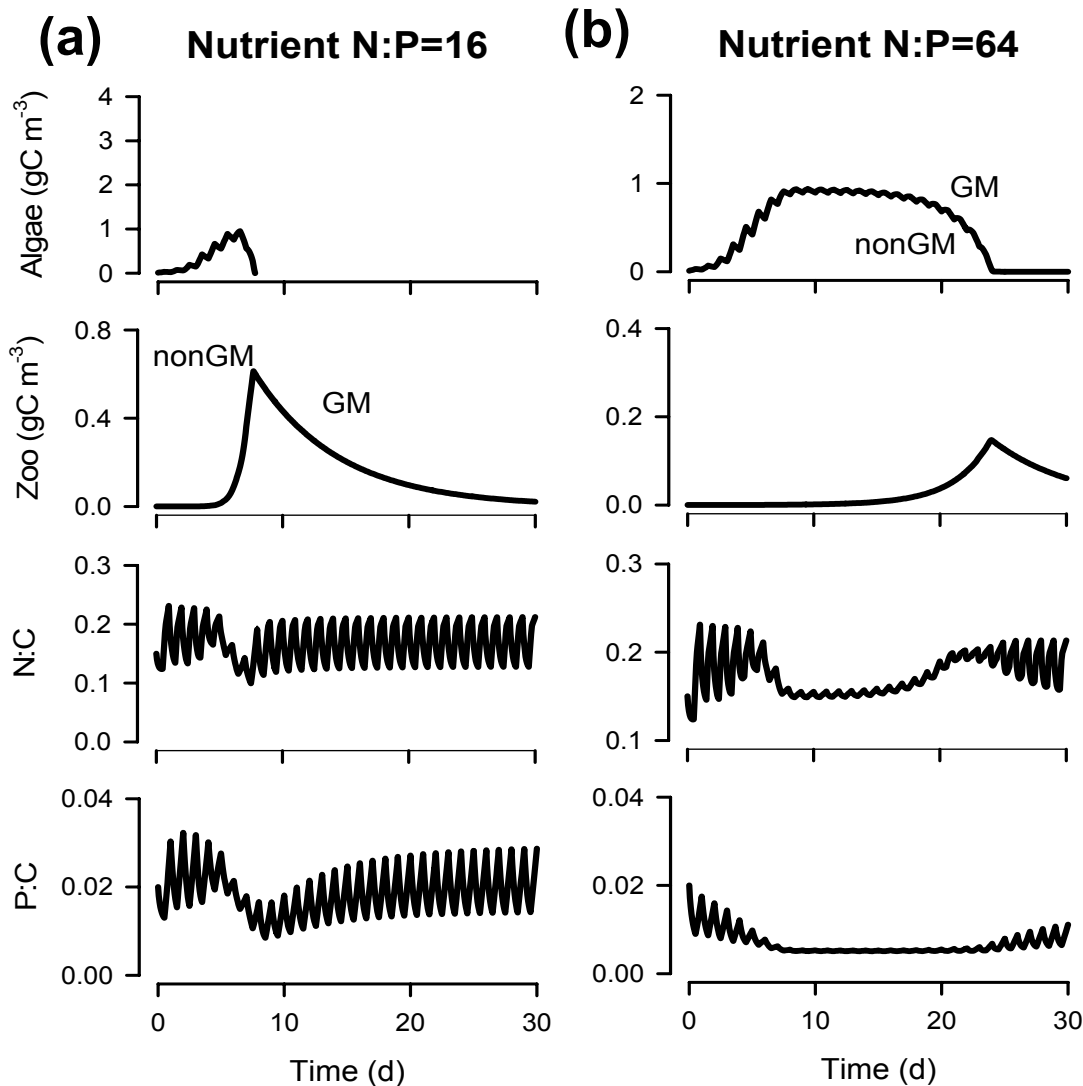


Figure S10. Simulated interaction between a microalga and its zooplanktonic predator. Simulations were run with the microalga configured to represent a non-GM or a GM strain with decreased NC₀. See table 2 for further details. In panel (a) the mole nutrient ratio is N:P 16, as expected in pristine water bodies. In panel (b) N:P is 64, representing the skewed nutrient content seen in eutrophic coastal waters. The temporal development of the interaction would depend on initial conditions. Plots show development of the algal and zooplankton biomass, and changes in the algal N:C and P:C ratios. Decreases in N:C and P:C indicate changes in nutrient stress (through exhaustion of external nutrient supply). There are essentially no points of difference between the non-GM and GM configurations.

GM PC_0

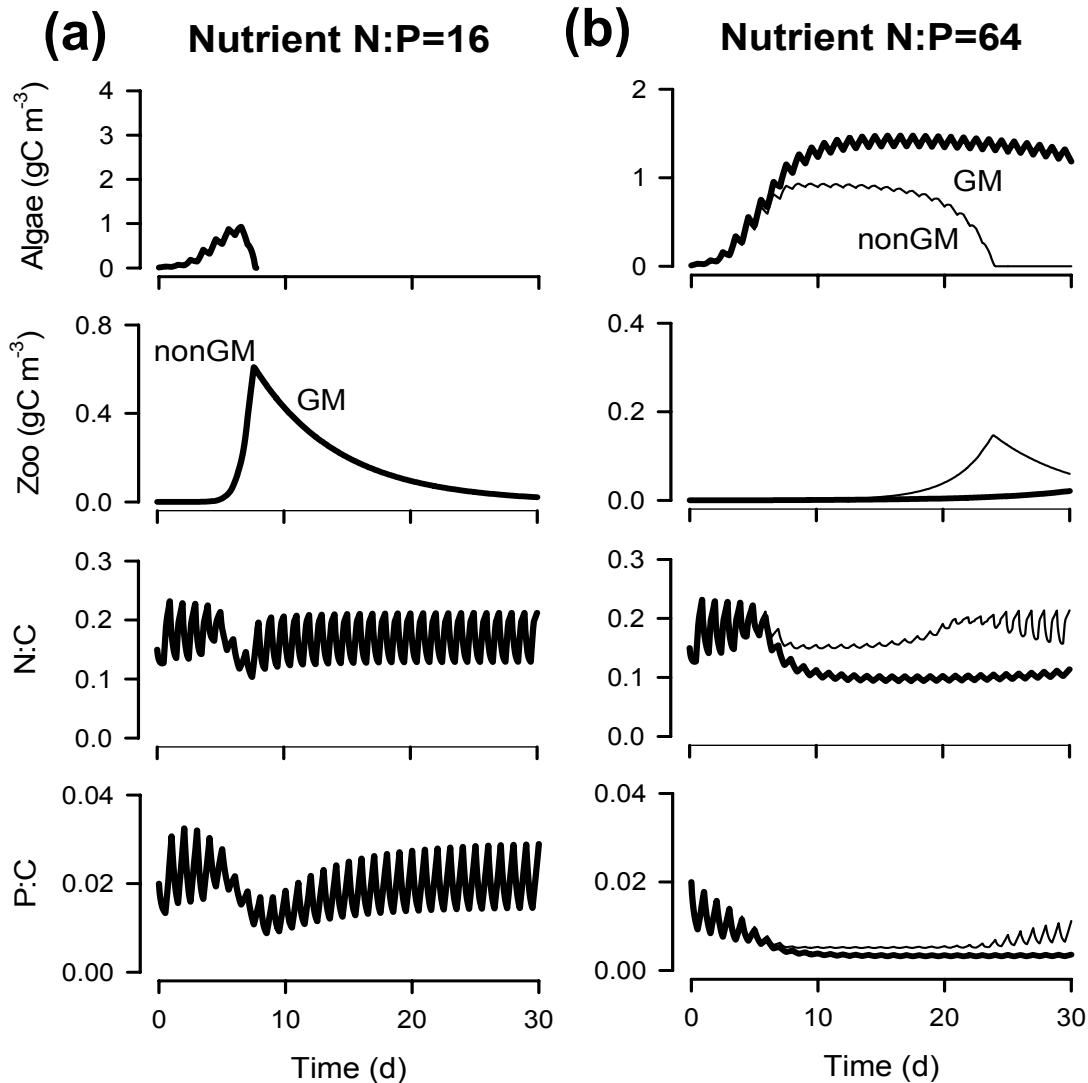


Figure S11. Simulated interaction between a microalga and its zooplanktonic predator. Simulations were run with the microalga configured to represent a non-GM or a GM strain with decreased PC_0 . See table 2 for further details. In panel (a) the mole nutrient ratio is N:P 16, as expected in pristine water bodies. In panel (b) N:P is 64, representing the skewed nutrient content seen in eutrophic coastal waters. The temporal development of the interaction would depend on initial conditions. Plots show development of the algal and zooplankton biomass, and changes in the algal N:C and P:C ratios. Decreases in N:C and P:C indicate changes in nutrient stress (through exhaustion of external nutrient supply).